

Oxygen and carbon isotope patterns in the Dicker Willem carbonatite complex, southern Namibia

David L. Reid^a and Alan F. Cooper^b

^aDepartment of Geochemistry, University of Cape Town, Rondebosch, 7700, South Africa

^bDepartment of Geology, University of Otago, Dunedin, New Zealand

(Received February 20, 1991; revised and accepted December 17, 1991)

ABSTRACT

Reid, D.L. and Cooper, A.F., 1992. Oxygen and carbon isotope patterns in the Dicker Willem carbonatite complex, southern Namibia. *Chem. Geol. (Isot. Geosci. Sect.)*, 94: 293–305.

Carbon and oxygen isotope data are presented for carbonatites and associated alkali silicate rocks from the Tertiary (49 Ma) Dicker Willem complex in southern Namibia. Carbonatites are grouped into: (1) coarse-grained sövites and associated silicate–oxide–phosphate-rich cumulates; (2) finer-grained alvikite intrusions, showing porphyritic and spinifex textures, comb layering and gravity-settled layers; (3) late-stage dykes, pipe breccias, veins and druses. The early sövites carry many inclusions of silicate rocks (ijolites, syenites). The most primitive carbon and oxygen isotope compositions are found in phenocrysts from calcite-phyric microsövite, bulk sövites and interstitial carbonate in the ijolites, with $\delta^{13}\text{C}$ (-5‰ vs. PDB) and $\delta^{18}\text{O}$ ($+7$ to $+9\text{‰}$ vs. SMOW). Oxygen isotope fractionation between cumulus pyroxene, magnetite and biotite in the sövites yields near magmatic temperatures of 600–900°C. Carbonates in some cumulates yield magmatic temperatures, but commonly show evidence of secondary alteration. Phenocrysts in dolomite-phyric alvikite are slightly enriched in ^{13}C (average $\delta^{13}\text{C} = -3.6\text{‰}$) and ^{18}O (average $\delta^{18}\text{O} = +9.9\text{‰}$) relative to primitive ratios, but taken together with data for phyric calcite define a linear trend of increasing $\delta^{13}\text{C}$ with $\delta^{18}\text{O}$ and can be modelled as being the product of combined carbonate–silicate–oxide–phosphate fractionation of a parent sövite. Groundmass carbonate in the porphyritic alvikites, as well as the bulk alvikites, all show variable degrees of ^{18}O enrichment relative to the phenocrysts, and reflect partial recrystallization of carbonate in the presence of low-temperature hydrous fluids.

1. Introduction

While few question the primary magmatic nature of most carbonatites, there is little consensus as to the composition of the original magma. Currently debated is the importance of alkali-poor carbonatite magmas (e.g., Gittins, 1989), given the undisputed existence of natural natro-carbonatite liquids (e.g., Dawson, 1989). Part of the problem is that most carbonatites are poorly preserved, preferentially weathered and eroded. Many carbonatites occur in partly exhumed intrusions, where available evidence bearing on the original magma is equivocal. Against this background of poor exposure and preservation, it is signif-

icant that newly discovered carbonatites in southern Namibia probably rank amongst the largest and best exposed in Africa, if not the world. The Dicker Willem carbonatite complex is not only characterised by excellent exposure, but it preserves features such as porphyritic and spinifex textures, igneous layering, crystal accumulation and other evidence for the existence of a mobile alkali-poor, Ca–Mg–Fe-carbonatite magma (Cooper, 1988; Cooper and Reid, 1991). In this paper we report and discuss results of a carbon and oxygen isotope study of a representative suite of carbonatites and associated silicate rocks (ijolites, syenites, trachytes) from Dicker Willem, as a further contribution to a series of recent papers deal-

ing with single complexes (Hubberten et al., 1988; Knudsen and Buchardt, 1991). Earlier reconnaissance studies of African carbonatites such as Deines and Gold (1973), Pineau et al. (1973), and Suwa et al. (1975) did not include Dicker Willem (or any other Namibian examples).

2. Geology

The Dicker Willem complex consists of several phases of intrusive carbonatite emplaced into high-grade gneisses of the Mid-Proterozoic Namaqua Province (Jackson, 1976; Cooper, 1988; Fig. 1). Associated silicate rocks are relatively minor and are confined to inclusions of ijolite and thin screens and sheets around the margins of the complex. Dated at 49 ± 2 Ma, the complex was emplaced during a fairly active period of Cretaceous–Tertiary alkaline activity in southern Namibia between 133 and 29 Ma (Reid et al., 1990). Two major carbonatite phases can be recognised: (1) an earlier series of coarse-grained sövites, which was intruded and disrupted by (2) multiple ring dykes of medium- to fine-grained alvikites (Cooper, 1988). Basement gneisses and granitoids are exposed discontinuously around the entire perimeter of the lower slopes and are faulted, brecciated, locally fenitized and intruded by peripheral plugs, dykes and concordant cone sheets of trachyte, various carbonatites and their explosively emplaced brecciated equivalents.

3. Petrography and mineralogy

3.1. Sövite

The early sövite intrusions consist of white calcite rocks with a variable but generally coarse grain size. The sövite can be traced as a coherent, concentric unit for up to 2.5 km along strike, particularly on the northeast and southwest slopes of Dicker Willem (Fig. 1). Elsewhere the sövite zone has been internally and

marginally disrupted, occurring as dispersed inclusions within banded alvikite. Near contacts with the country rock, minor intrusions of calcite-phyric microsövite occur, which probably represent rapidly cooled equivalents of the sövitic magma. Calcite phenocrysts are typically tabular, and reach large dimensions (3–4 cm long) and are composed of almost pure CaCO_3 , but with up to 1.1% SrO (Cooper and Reid, 1991).

Sövites contain euhedra of magnetite, a clinopyroxene zoned from aegirine–augite cores to aegirine rims, and pyrochlore, together with tabular biotite and rounded prisms of apatite set in a granular to bladed aggregate of calcite. Some sövites also carry melanite and nepheline. No dolomite is present. The order of crystallization inferred from thin section is generally magnetite, followed by Na-augite, biotite, pyrochlore and finally calcite. Apatite appears to crystallize throughout the sequence.

The sövite contains irregular segregations or pods, sometimes up to 60 m in length, comprising accumulations of magnetite, Na-augite, biotite, pyrochlore and apatite. On the basis of the deduced order of crystallization these segregations are interpreted as sövite cumulates. Sample AFC-090 is a pyroxene cumulate with close-packed euhedral crystals of green aegirine–augite ($\text{Di}_{42}\text{Hd}_{14}\text{Ac}_{44}$), cemented by intercumulus calcite. A more complex cumulate is represented by sample AFC-213, which contains roughly equal proportions of magnetite, biotite, Na-augite ($\text{Di}_{58}\text{Hd}_{23}\text{Ac}_{19}$) and apatite. Accessory pyrochlore also occurs as small euhedra, and is probably also an early cumulus phase.

3.2. Ijolite inclusions

The sövite is also characterised by numerous inclusions of texturally heterogeneous, coarse- to medium-grained silicate rocks, which comprise various types of ijolites. Replacement of feldspathoid with K-feldspar is seen in some samples, and may represent a metaso-

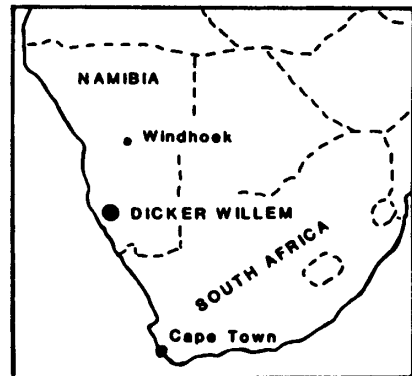
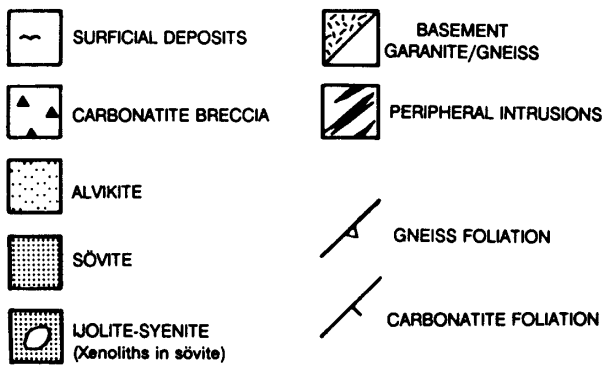
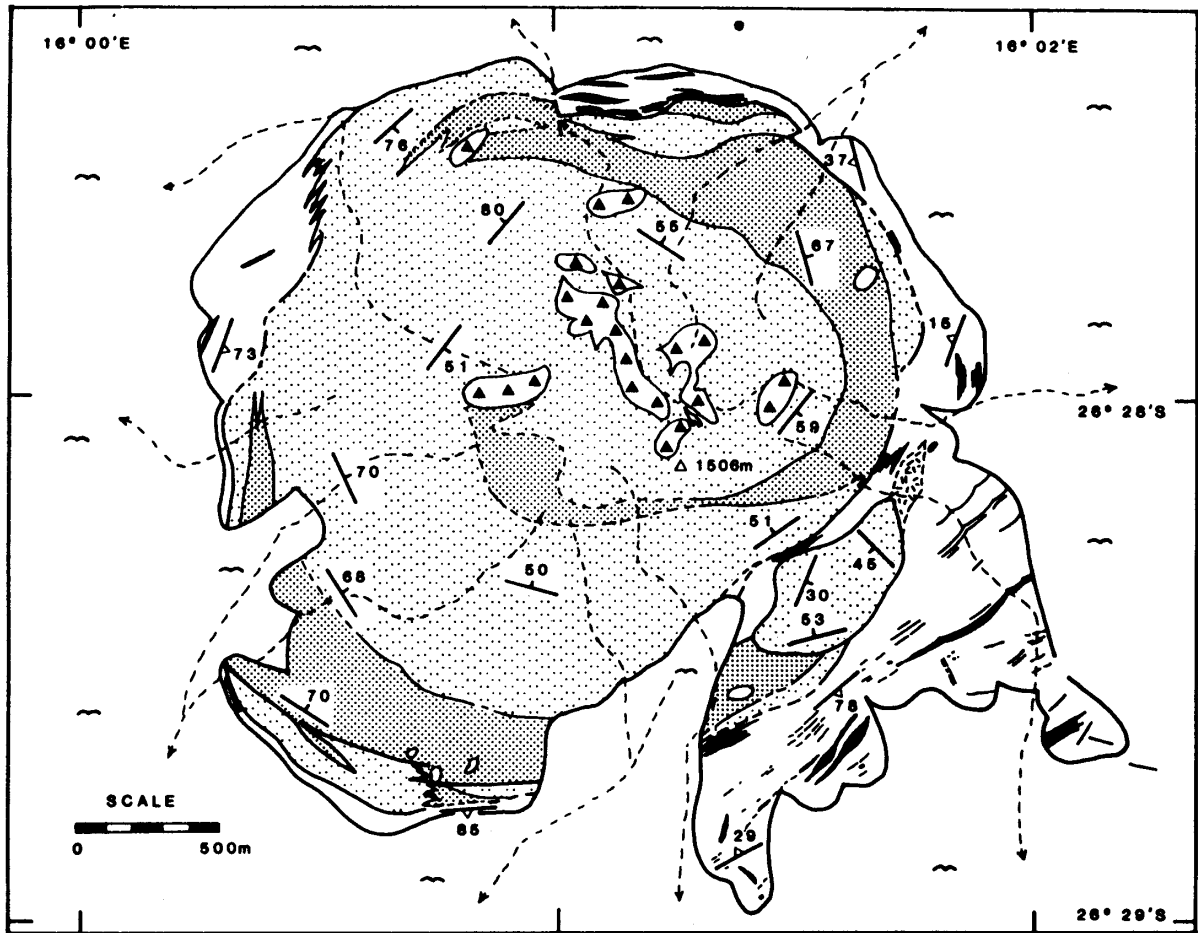


Fig. 1. Geological map of the Dicker Willem carbonatite complex, southwestern Namibia.

matic reaction towards syenites (potassic fenites?). Apart from nepheline, the ijolites contain variable quantities of green aegirine-

augite, brown melanite, brown biotite, K-feldspar and calcite. One variety of ijolite (samples AFC-085 and -086) contains significant

quantities of wollastonite. Mineral compositions of the ijolites overlap with silicates found in the sövites. For example, pyroxene, biotite and nepheline compositions in ijolite AFC-068, are practically identical with sövite AFC-093, perhaps indicating that their bulk compositions represent immiscible fractions (Cooper and Reid, 1991).

Many ijolites contain interstitial carbonate (up to 20 wt% judging from measured CO₂ contents), which appears texturally primary, in the sense that it has crystallized against euhedral crystal faces of coexisting pyroxene, biotite and nepheline. Samples of ijolite taken for analysis were chosen from the interiors of inclusions, in order to avoid contact effects with the host sövite. Certainly the margins of many ijolite inclusions show evidence of introduced carbonate along micro-veins and fractures developed in the silicate and oxide minerals.

3.3. Alvikite

The alvikites at Dicker Willem are fine-grained, buff to pale brown, occasionally banded and/or porphyritic calcite carbonatites that intrude the basement gneisses and sövite zone as moderately to steeply dipping concentric cone sheets and ring dykes and occasional cross-cutting dykes. Although alvikites are mineralogically diverse, the fine-scale interbanding prevents further subdivision of mapped units.

Porphyritic alvikites contain phenocrysts of magnetite, pyrochlore and rhombic ferroan, manganian dolomite (average composition Ca_{52.0}Mg_{42.7}Fe_{2.5}Mn_{1.5}Sr_{1.3}). Groundmass textures vary from granular to distinctly spinifex-like, with the latter being composed of an intricate bladed intergrowth of calcite and less abundant dolomite. The original bladed calcite-dolomite assemblage is commonly pseudomorphed by finer-grained granular aggregates, suggestive of sub-solidus recrystallization, which also imparts a turbid brown colour to the dolomite. A similar secondary al-

teration is developed as rims around the larger dolomite phenocrysts.

A feature of the dolomite- and magnetite-phyric alvikites is the highly variable concentration and distribution of the phenocrysts. Phenocrysts may occur in cumulate layers, or irregular trains, clusters or folded bands. Dolomite phenocrysts occur as creamy white rhombs when fresh, but alter to brown limonitic pseudomorphs when altered.

3.4. Late-stage carbonates

Late-stage carbonates include: (1) brown dykes that cut the alvikites, but which are truncated by the breccia pipes; (2) yellow veins associated with the breccia pipes; (3) a post-breccia dolomite carbonatite dyke; and (4) post-breccia veins and pods of very coarse white drusy carbonate. The brown dykes were initially regarded as ferro-carbonatites and thought to be composed of ankerite or even siderite. Inspection under the microscope and in the laboratory showed the dark carbonate to be calcite intricately veined with hydrated iron oxides. Both brown and yellow carbonates are simply granular or rarely pilotaxitic laths of medium- to fine-grained calcite showing different intensities of Fe-staining. Chemically, both brown and yellow dykes contain similar amounts of total Fe and Mn, and their different appearances may be just the degree of oxidation.

The drusy carbonate is calcite, showing variable grain size and habit, with margins of the body commonly showing centimetre-scale banding parallel to the walls. Centres of several druses have crystallized as aggregates of very coarse divergent calcite blades up to 20 cm long. Field relations suggest deposition from circulating hydrothermal solutions.

4. Results

4.1. Methods

Oxygen and carbon isotope data for carbonate and selected silicates and oxides are listed

TABLE 1

Carbon and oxygen isotope data for carbonatites

Sample	Description	δ ¹³ C (‰ vs. PDB)	δ ¹⁸ O (‰ vs. SMOW)
<i>Sövite intrusion:</i>			
AFC-093	Cpx-Neph-Mel sövite	-5.1	+8.0
AFC-084	Biot-Apt sövite	-4.8	+9.3
AFC-071	Cpx sövite inclusion in alvikite	-5.0	+10.6
AFC-154	sövite dyke	-3.6	+5.5
AFC-213	Mt-Cpx-Biot-Apt cumulate in sövite	-2.0	+22.0
AFC-213* ¹	magnetite	-2.6	+20.7
	clinopyroxene		+1.6
	biotite		+5.3
AFC-132	Mt-rich cumulate in sövite	-6.9	+24.0
DLR-A* ²	magnetite sövite inclusion in alvikite	-5.1	+3.2 +8.5
DLR-A* ¹		-5.2	+7.9
DLR-E* ¹	sövite inclusion in alvikite	-5.1	+7.7
AFC-090* ¹	sövite cumulate clinopyroxene	-5.1	+7.1 +5.7
<i>Alvikite intrusive complex:</i>			
AFC-242	Dol-phyric alvikite (spinifex matrix)	-3.6	+13.0
	dolomite phenocryst	-4.4	+9.2
	groundmass calcite	-3.2	+11.9
AFC-92A	Dol-phyric alvikite (spinifex matrix)		
	dolomite phenocryst	-3.5	+9.6
	groundmass calcite	-2.2	+9.3
AFC-031	Dol-phyric alvikite (granular matrix)	-3.2	+13.1
	dolomite phenocryst	-3.3	+10.6
	groundmass calcite	-3.2	+12.9
AFC-043	Dol-phyric alvikite	-2.9	+14.8
AFC-238	Dol-phyric alvikite	-3.4	+17.7
AFC-253	Dol-phyric alvikite	-3.1	+17.0
DLR-C* ²	alvikite	-4.0	+17.9
DLR-C* ¹		-4.0	+17.6
DLR-1* ¹	alvikite	-2.1	+11.7
AFC-149	dolomite cumulate	-3.2	+17.1
AFC-256	dolomite cumulate	-4.4	+17.3
AFC-009	spinifex alvikite	-2.7	+16.2
AFC-254	spinifex alvikite	-2.6	+16.2
AFC-005	Cal-phyric alvikite	-4.1	+13.4
AFC-018	Cal-phyric alvikite	-4.7	+13.9
AFC-051	Cal-phyric alvikite	-4.5	+13.2
	calcite phenocryst	-5.5	+7.0
	groundmass calcite	-5.6	+13.9
AFC-112	Cal-phyric alvikite	-3.7	+17.4
	calcite phenocryst	-5.0	+7.5
	groundmass calcite	-3.5	+17.7

TABLE 1 (continued)

Sample	Description	δ ¹³ C (‰ vs. PDB)	δ ¹⁸ O (‰ vs. SMOW)
<i>Alvikite intrusive complex (cont.):</i>			
AFC-217	Dol-phyric alvikite (spinifex matrix)	-2.6	+13.5
	dolomite phenocryst	-3.1	+10.2
	groundmass calcite	-2.1	+11.1
AFC-025	Dol-phyric alvikite	-3.4	+15.0
AFC-200	alvikite	-3.6	+13.6
AFC-028	Mt-phyric alvikite	-4.0	+17.4
AFC-182	alvikite	-3.7	+19.4
AFC-022	alvikite	-3.3	+15.3
DLR-B	alvikite	-3.3	+14.7
DLR-B* ¹		-3.7	+13.8
AFC-036	Mt-phyric alvikite	-3.1	+15.3
	magnetite		+0.04
AFC-049	Mt-phyric alvikite	-3.3	+17.4
	magnetite		-0.8
AFC-246	Mt-phyric alvikite	-6.4	+24.5
	magnetite		+0.4
AFC-074	alvikite	-3.2	+25.3
AFC-078	alvikite	-3.7	+14.2
AFC-188	alvikite	-3.5	+17.0
AFC-193	alvikite	-3.6	+16.2
<i>Late brown dykes:</i>			
AFC-060		-7.7	+25.3
AFC-073		-8.0	+25.3
AFC-173		-6.9	+25.5
DLR-2* ¹		-6.2	+26.8
<i>Yellow veins associated with breccia pipes:</i>			
AFC-055		+0.3	+27.8
AFC-056		-6.3	+25.3
AFC-257		+0.8	+28.7
AFC-258		-2.0	+26.6
AFC-138		-6.6	+24.1
AFC-087	dolomite dyke	-1.9	+14.1
<i>Drusy calcite pods and veins:</i>			
DLR-3	fine-grained selvage	-7.0	+25.9
DLR-4	banded marginal zone	-7.0	+25.1
DLR-7	coarse bladed interior	-6.7	+24.1
DLR-6	calcrete on alvikite	-1.8	+29.2
<i>Country-rock marbles:</i>			
AFC-220	coarse marble	+0.03	+15.5
AFC-221	banded forsterite marble		
	subzone 1	-1.5	+8.6
	subzone 2	-1.4	+9.5
	subzone 3	-1.6	+7.9
	subzone 4	-1.3	+10.4

Apt=apatite; Biot=biotite; Cal=calcite; Cpx=clino-pyroxene; Dol=dolomite; Mel=melilite; Mt=magnetite; Neph=nepheline.

*¹Hand-picked carbonate. *²Whole-rock powder.

in Tables 1 and 3. Techniques employed for carbonates are based on McCrea (1950) and Sharma and Clayton (1965). Silicates and oxides were analysed using the methods of Venemann and Smith (1990). All oxygen isotope ratio measurements were normalised to V-SMOW, and $\delta^{18}\text{O}$ for NBS-28 of +9.64‰. Carbon isotope ratios are reported relative to PDB. Analytical uncertainty in both $\delta^{13}\text{C}$ and $\delta^{18}\text{O}$ is estimated at $\pm 0.2\text{‰}$.

The majority of carbonate analyses was carried out on a $\sim 200\text{-}\mu\text{m}$ size fraction prepared from a whole-rock crush. The size fraction was rinsed in double-distilled water to remove dust-sized particles prior to analysis. No attempt to separate the carbonate fraction was made before analysis, except in the case of the phenocryst-groundmass study, where carbonate was hand-picked.

4.2. Porphyritic carbonatites

Data for hand-picked phenocrysts (dolomite or calcite), hand-picked groundmass calcite and bulk samples, are listed in Table 1. Calcite phenocrysts have C and O isotope values ($\delta^{13}\text{C}$ -5.5 to -5.0‰ , average -5.3‰ ; $\delta^{18}\text{O}$ $+7.0$ to $+7.5\text{‰}$, average $+7.3\text{‰}$) which closely resemble those established for primary magmatic carbonatites derived from the mantle (Fig. 2), while the dolomites appear to be displaced to higher $\delta^{13}\text{C}$ (-4.4 to -3.1‰ , average -3.6‰) and $\delta^{18}\text{O}$ ($+9.2$ to $+10.6\text{‰}$, average $+9.9\text{‰}$). Variation in $\delta^{13}\text{C}$ and $\delta^{18}\text{O}$ appears to be correlated, and the trend (hereafter called the "phenocryst array") yields a slope of ~ 0.65 . Groundmass calcites in the calcite-phyric carbonatites are strongly enriched in ^{18}O ($\delta^{18}\text{O}$ $+13.9$ to $+17.7\text{‰}$, average $+15.8\text{‰}$), but show little change in $\delta^{13}\text{C}$ (average -4.6‰ compared with -5.3‰ for the phenocrysts). Clearly the groundmass calcite does not retain a primary oxygen isotope composition.

No consistent pattern can be identified in the dolomite-bearing carbonatites, with ground-

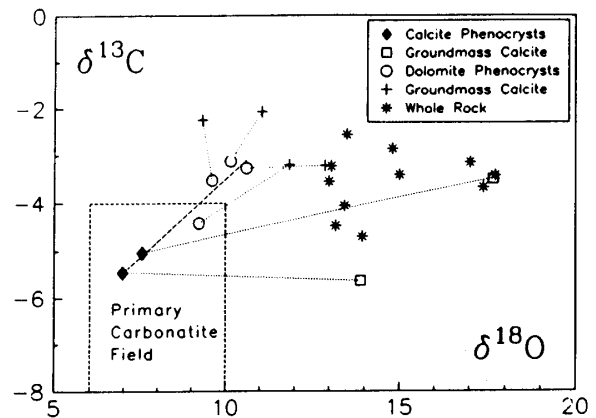


Fig. 2. Plot of $\delta^{13}\text{C}$ (vs. PDB) against $\delta^{18}\text{O}$ (vs. SMOW) for phenocrysts in porphyritic carbonatites, their coexisting calcitic groundmasses, and dolomite cumulates. Dotted tie-lines join phenocrysts with coexisting calcitic groundmasses. The dashed box is the field estimated for primary magmatic carbonatites after Taylor et al. (1967). The best-fit line through the calcite and dolomite phenocrysts (called here the phenocryst array) yields a slope of ~ 0.65 .

mass calcite showing enrichment in ^{18}O relative to the phenocrysts, with AFC-92A being the exception. Average $\delta^{13}\text{C}$ for the groundmass is -2.7‰ , and average $\delta^{18}\text{O}$ is $+11.3\text{‰}$. The groundmass is also slightly enriched in ^{13}C , but parallel to the phenocryst array. Carbon and oxygen isotope fractionations between dolomite and groundmass calcite are not large ($< 2\text{‰}$), but tend to be the reverse of that predicted by Deines (1989), so that it is not possible to estimate temperatures. The pattern of carbon and oxygen isotope partitioning between dolomite and calcite phenocrysts is in the right sense (i.e. dolomite enriched in ^{13}C and ^{18}O), but these minerals do not coexist in the same rock and consequently any temperature estimate may not be valid.

In addition to porphyritic carbonates, two samples interpreted to be dolomite cumulates (samples AFC-149 and -256), have also been plotted in Fig. 2. However, they show extreme ^{18}O enrichment (average $\delta^{18}\text{O} = +17.2\text{‰}$), similar to that observed for some groundmass carbonate, as well as the majority of bulk alvikite samples described on p.300. The two sam-

ples showed strong limonitic staining along grain boundaries and closely spaced fractures, and appear to have suffered secondary alteration.

4.3. Sövites

4.3.1. Cumulate rocks. Measured values for $\delta^{18}\text{O}$ in the pyroxene and calcite from cumulate rock AFC-090 are listed in Table 1, and yield a Δ of 1.4‰ (Table 2), corresponding to a magmatic equilibrium temperature of $> 800^\circ\text{C}$, using estimated inter-mineral fractionation curves summarised in Deines (1989). The calcite has a $\delta^{13}\text{C}$ of -5.1‰ and $\delta^{18}\text{O}$ of $+7.1\text{‰}$, which plot in the primary magmatic field very close to those obtained for the calcite phenocrysts (Fig. 2) and the bulk sövites (Fig. 3).

Isotopic data for cumulate rock AFC-213 are listed in Table 1, while calculated inter-mineral fractionation temperatures (based on Deines, 1989) are given in Table 2. The magnetite-clinopyroxene temperature appears

TABLE 2

Inter-mineral oxygen isotope fractionation data and isotopic temperatures, using the curves in Deines (1989)

Sample	Mineral pair	Δ	T ($^\circ\text{C}$)
AFC-090	clinopyroxene-calcite	1.4	> 800
AFC-213	magnetite-clinopyroxene	3.6	> 800
	magnetite-biotite	4.5	~ 600
	biotite-clinopyroxene	0.9	~ 600
	calcite-clinopyroxene	15.5	< 200
	calcite-magnetite	19.1	< 200
	calcite-biotite	14.6	< 200
AFC-132	calcite-magnetite	24.0	< 200
AFC-036	calcite-magnetite	15.3	~ 200
AFC-049	calcite-magnetite	17.4	< 200
AFC-246	calcite-magnetite	24.5	< 200
<i>Combined estimates:</i>			
AFC-051/AFC-213	calcite-magnetite	5.3	> 800
AFC-051/AFC-132	calcite-magnetite	3.8	> 800
AFC-242/AFC-246	dolomite-magnetite	8.8	~ 520

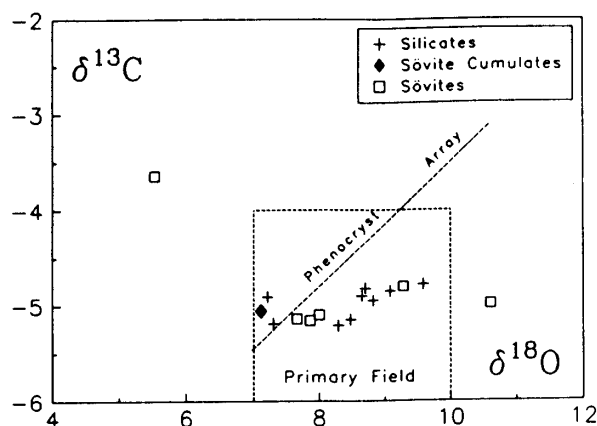


Fig. 3. Plot of $\delta^{13}\text{C}$ against $\delta^{18}\text{O}$ for bulk carbonatite samples (sövites, sövite cumulates and interstitial carbonate in silicate rocks) from the Dicker Willem complex. The phenocryst array is from Fig. 2.

magmatic ($> 800^\circ\text{C}$), while biotite-magnetite and biotite-clinopyroxene temperatures are somewhat lower ($\sim 600^\circ\text{C}$), perhaps suggestive of continued closed system sub-solidus exchange involving biotite. Mineral pairs involving calcite yield very low apparent temperatures ($< 200^\circ\text{C}$). Clearly the carbonate in this rock has suffered secondary ^{18}O enrichment.

A third cumulate rock (AFC-132) consists mainly of subhedral magnetite crystals cemented with calcite, which also shows strong enrichment in ^{18}O ($\delta^{18}\text{O} = +24.0\text{‰}$), and predictably yields a very low apparent temperature when compared with the observed $\delta^{18}\text{O}$ of the magnetite ($+3.2\text{‰}$, Table 2). Higher temperatures are obtained when combining the magnetite $\delta^{18}\text{O}$ data with those obtained for the calcite phenocrysts in associated carbonatite intrusions (Table 2). While not strictly speaking a coexisting mineral pair, the data do indicate that magnetite retains a magmatic isotopic signature.

4.3.2. Bulk sövites. Sövites containing only minor quantities of silicates have been analysed

as bulk samples and their compositions (average $\delta^{13}\text{C} = -5.0\text{‰}$, average $\delta^{18}\text{O} = +8.4\text{‰}$) plot very close to those of the calcite phenocrysts, perhaps suggesting that these rocks may actually represent cumulates (Fig. 3). Variation in $\delta^{13}\text{C}$ is slight, but there is some dispersion in $\delta^{18}\text{O}$ from typical mantle values of +6–8‰, up to +10‰. Only a discrete sövite dyke in the country rock (AFC-154) has a different composition, with isotopically heavier carbon.

4.4. Alvikites

4.4.1. Magnetite alvikites. Apart from the magnetite-rich sövite described on p.299, three magnetite-phyric alvikites have been studied, and their oxygen and carbon isotope compositions are listed in Table 1. Magnetite–calcite pairs yield Δ -values between 15 and 24‰ (Table 2), indicative of very low apparent equilibration temperatures (<200°C). Again it would appear from the observed $\delta^{18}\text{O}$ -values in the carbonate (+15 to +25‰), that secondary alteration has occurred. Assuming the average magnetite $\delta^{18}\text{O}$ of -0.1‰ from the three samples to be close to the primary magmatic value, then some estimate of the $\delta^{18}\text{O}$ in a coexisting carbonatite magma could be made. Judging from the magnetite–calcite equilibrium fractionation curve published in Deines (1989), a carbonatite magma in equilibrium with such a magnetite would have a $\delta^{18}\text{O}$ -value of +5 to +7‰, in the temperature range of 800–600°C. Such a $\delta^{18}\text{O}$ is close to that observed for the sövites.

4.4.2. Bulk alvikites. Compared with the sövites, the alvikites are distinctly enriched in ^{18}O and ^{13}C , so that they occupy a separate field in Fig. 4. Compared with the phenocryst array, the alvikites as a group show simply a displacement to higher $\delta^{18}\text{O}$, with some samples having values as heavy as +18‰. Predictably the bulk alvikites are isotopically similar to the groundmass carbonate measured in the porphyritic varieties. On average, the alvikites

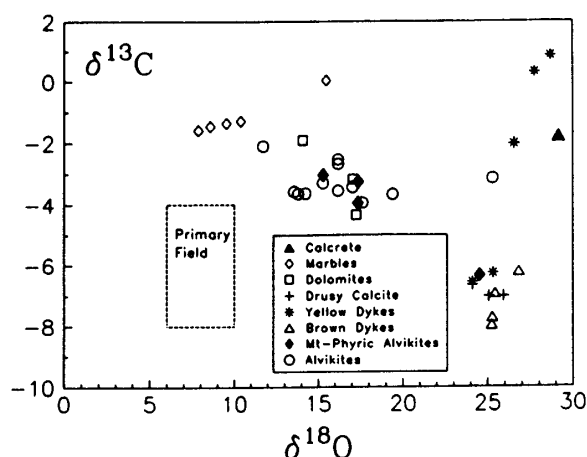


Fig. 4. Plot of $\delta^{13}\text{C}$ against $\delta^{18}\text{O}$ for bulk carbonatite samples (alvikites, late-stage dykes and veins) from the Dicker Willem complex.

have $\delta^{13}\text{C} = -3.4\text{‰}$ and $\delta^{18}\text{O} = +15.3\text{‰}$, compared to the sövites with -5.0‰ and $+8.4\text{‰}$, respectively. Alvikites with $\delta^{18}\text{O}$ -values of $> +20\text{‰}$ resemble the late-stage veins plotted in Fig. 4, and which are described in the next section.

4.5. Late-stage dykes and veins

Brown dykes cut the alvikite sub-complex, but are themselves truncated by the yellow carbonatite breccias. Four dykes analysed all show strong ^{18}O enrichment ($\delta^{18}\text{O}$ up to +27‰, average +25.7‰), as well as having the lowest $\delta^{13}\text{C}$ -values (-8 to -6‰ , average -7.2‰) encountered at Dicker Willem (Fig. 4).

Yellow veins of carbonatite cross-cut sövites, alvikites, brown carbonate dykes, as well as impart the same colour to the matrix of the breccia pipes. Post-breccia yellow veins also occur. Isotope compositions vary widely, although most samples are characterised by very high $\delta^{18}\text{O}$ ($> +25\text{‰}$, average +26.5‰). Another interesting feature is the very wide range in $\delta^{13}\text{C}$ (-8 to 0‰ , Fig. 2), with yellow vein

carbonatite defining the upper and lower extremes observed at Dicker Willem.

Calcite was collected from the fine-grained selvage of a druse (DLR-3), granular banded zones developed parallel to the margins (DLR-4) and the coarse-bladed interior (DLR-7). All samples from the druse have high $\delta^{18}\text{O}$ (average = +25.1‰) and low $\delta^{13}\text{C}$ (average = -6.9‰), and therefore show degrees of ^{13}C depletion noted for some of the yellow carbonatite veins (Fig. 3).

Many surface outcrops of igneous carbonatite are mantled by encrustations of white powdery calcite, which also cements the wide talus fans that emanate from the inselberg forming Dicker Willem. The very high $\delta^{18}\text{O}$ of +29.2‰ is to be expected, while the $\delta^{13}\text{C}$ -value of -1.8‰ is intermediate, when compared to data obtained for the late-stage carbonatite veins (Fig. 4).

4.6. Silicate rocks

Isotopic compositions of interstitial carbonate in silicate rocks are listed in Table 3. Interestingly the isotopic data practically coincide

TABLE 3

Carbon and oxygen isotope data for carbonate in silicate rock types

Sample	Rock	$\delta^{13}\text{C}$ (‰ vs. PDB)	$\delta^{18}\text{O}$ (‰ vs. SMOW)
AFC-068	Cpx-Mel ijolite	-5.21	+8.29
AFC-081	Cpx syenite	-4.95	+8.82
AFC-082	Cpx syenite	-4.78	+9.58
AFC-083	Cpx ijolite	-5.15	+8.48
AFC-085*	Wol ijolite	-4.91	+7.21
AFC-086*	Wol ijolite	-5.19	+7.30
AFC-095	Cpx ijolite	-4.85	+9.08
AFC-095	Cpx ijolite	-4.82	+8.70
AFC-232	Cpx ijolite	-4.90	+8.65
AFC-233	fenitized granite	-3.58	+14.38
AFC-201			
AFC-010	K-trachyte dyke	-2.35	+15.24

Cpx = clinopyroxene; Mel = mellilite; Wol = wollastonite.

*Hand-picked carbonate.

with the field occupied by the bulk sövites and calcite phenocrysts (Fig. 3) and therefore exhibit a primitive magmatic signature (average $\delta^{13}\text{C} = -5.0‰$, $\delta^{18}\text{O} = +8.4‰$). The only silicate rocks that plot away from the primary magmatic field are a fenitized granitoid (AFC-201) with $\delta^{18}\text{O}$ of +14.4‰ and a K-trachytic breccia dyke in the surrounding country rock (AFC-010) with a $\delta^{18}\text{O}$ of +15.2‰, which are clearly distinct from the ijolitic inclusions.

4.7. Country-rock marbles

A coarse-grained marble from the Garub Group which has been described as metamorphosed to granulite-facies grade (Jackson, 1976) has a $\delta^{13}\text{C}$ -value of 0‰, which probably reflects its sedimentary heritage and distinguishes these country-rock marbles from the carbonatites (Fig. 4). Its $\delta^{18}\text{O}$ -value of +15.5‰ is low for sedimentary carbonates but in view of the high metamorphic grade, partial equilibration with a metamorphic fluid cannot be ruled out. Data for an impure marble composed of calcite and serpentinised olivine show little change in $\delta^{13}\text{C}$ (-1.6 to -1.4‰), but there was a slight variation in $\delta^{18}\text{O}$ (+7.8 to +10.4‰).

5. Discussion

Inspection of the range in C and O isotope composition of Dicker Willem carbonatites reveals certain patterns, which can be described as follows:

(1) The linear trend defined by the calcite and dolomite phenocryst data. This is termed the "phenocryst array" and has a slope of ~0.65.

(2) The coincidence of isotopic compositions for the bulk sövites, calcite phenocrysts, intercumulus calcite in a sövite cumulate and interstitial calcite in the ijolites. The field so defined falls within that established for mantle-derived carbonatites (Taylor et al., 1967).

(3) Displacement of the bulk alvikites from

the phenocryst array towards higher $\delta^{18}\text{O}$.

(4) Veins of brown and yellow carbonate, carbonatite breccias, drusy cavities and calcite encrustations, showing the highest observed $\delta^{18}\text{O}$ -values, but with highly variable $\delta^{13}\text{C}$ spanning a wide range from -8 to 0 ‰.

5.1. Origin of the phenocryst array

Although not strictly coexisting, the average $\delta^{13}\text{C}$ - and $\delta^{18}\text{O}$ -values for the calcite (-5.3 ‰ and $+7.3$ ‰, respectively) and dolomite (-3.6 ‰ and $+9.9$ ‰, respectively) are too different to permit explanation simply by equilibrium fractionation of carbon and oxygen isotopes. It could be argued that the calcite- and dolomite-phyric carbonatites simply represent distinct magmas with different $\delta^{13}\text{C}$ and $\delta^{18}\text{O}$. However, these rock types have similar initial Sr and Nd isotopic compositions (D.L. Reid and A.F. Cooper, unpublished data, 1990), which argue for them being comagmatic.

Taking the extreme values, the phenocryst array involves a change in $\delta^{13}\text{C}$ from -5.5 to -3.4 ‰ and $\delta^{18}\text{O}$ from $+7.0$ to $+10.5$ ‰ (Fig. 2). Such positive correlation between $\delta^{13}\text{C}$ and $\delta^{18}\text{O}$ appears common (Deines, 1989), and several models have been proposed to account for such a relationship. Pineau et al. (1973) have modelled ^{13}C and ^{18}O enrichment in carbonate precipitating from a magma under closed-system conditions where CO_2 is the dominant oxygen (and carbon) carrier. Model curves are plotted in Fig. 5, assuming that fractionation of carbon and oxygen isotopes occurred between calcite and CO_2 at 700°C . Fractionation factors at this temperature (after Bottinga, 1968) are: $\alpha^{13}\text{C}=0.9978$, $\alpha^{18}\text{O}=0.9945$. Starting with a primary isotope composition similar to that observed for the lower end of the phenocryst array ($\delta^{13}\text{C}=-5.5$ ‰, $\delta^{18}\text{O}=+6.9$ ‰), increase in $\delta^{13}\text{C}$ and $\delta^{18}\text{O}$ can be achieved at advanced stages of differentiation (Fig. 5). The slope of ^{13}C and ^{18}O enrichment can be modified by admitting

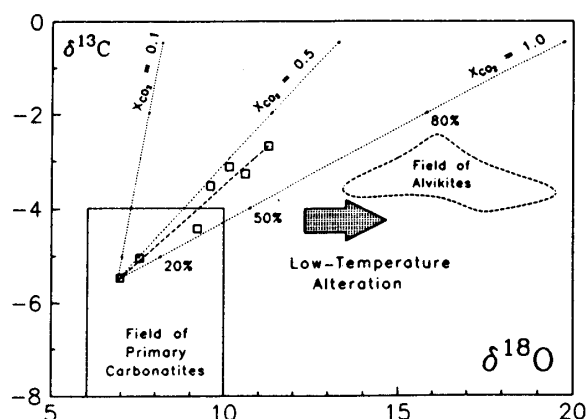


Fig. 5. Plot of $\delta^{13}\text{C}$ against $\delta^{18}\text{O}$ showing the phenocryst array compared with model curves for closed-system carbonate crystallization (after Pineau et al., 1973). Percentage labels represent degree of fractional crystallization of carbonatite magma. Numeric labels at the top of each curve indicate the X_{CO_2} in the reservoir (in terms of oxygen content).

variable proportions of H_2O as an additional oxygen carrier, which effectively reduces the degree of fractionation of oxygen isotopes between calcite and its reservoir ($\alpha^{18}\text{O}_{\text{calcite-H}_2\text{O}}$ at $700^\circ\text{C} \approx 1.0000$). The best fit appears to involve a reservoir with a $\text{CO}_2/\text{H}_2\text{O}$ ratio (in terms of oxygen content) of 1:1 (equivalent to $X_{\text{CO}_2}=0.5$). Pineau et al. (1973) and Deines (1989) note that the average slope of many carbonatite complexes in terms of $\delta^{13}\text{C}$ - $\delta^{18}\text{O}$ variation is ~ 0.4 , which is significantly lower than for the Dicker Willem array. Correspondingly Pineau et al. (1973) restricted the amount of oxygen present in the form of H_2O (or silicates) to $< 30\%$. The steeper Dicker Willem trend does not require such a restriction, and it is noted that several carbonatite complexes described by Deines (1989) do show steeper trends of $\delta^{13}\text{C}$ - $\delta^{18}\text{O}$ variation, particularly at lower $\delta^{18}\text{O}$ -values.

The model curves shown in Fig. 5 have been constructed assuming calcite-fluid equilibrium partitioning, and allowance must be made for the fact that dolomite and not calcite must control fractionation in the latter stages. Values of $\alpha^{13}\text{C}$ and $\alpha^{18}\text{O}$ for dolomite are slightly

less than calcite, so increases in $\delta^{13}\text{C}$ and $\delta^{18}\text{O}$ will not be so large, but the slope of the curves would not be greatly modified.

Another complicating factor is that the sequence of intrusion of Dicker Willem carbonatites is calcite-phyric, followed by dolomite-phyric varieties. According to experimental work of Fanelli et al. (1986) at 2 kbar, possible isobaric crystallization histories involve liquidus sequences of calcite, calcite + dolomite and calcite + dolomite + periclase *or* dolomite, dolomite + periclase and dolomite + calcite + periclase. In order to cause dolomite to *replace* calcite as the sole liquidus phase, it must be postulated that the melt was subjected to a change in conditions that expanded the field of dolomite at the expense of calcite. No experimental work appears to have been carried out on factors controlling such field-boundary changes (total pressure, $P_{\text{H}_2\text{O}}$, P_{CO_2} , etc.), but it is suggested that in the evolution from calcite-phyric to dolomite-phyric carbonatite, some extensive parameter was affected.

Finally, the Dicker Willem sövites also carry silicates, magnetite and apatite, any or all of which may have fractionated, and therefore contributing to the observed pattern of ^{18}O enrichment.

5.2. Origin of the ^{18}O -enriched bulk alvikites

Evidence for ^{18}O enrichment of the groundmasses in calcite and some dolomite-phyric carbonatites has already been described. This isotopic shift appears to be related to partial replacement of primary igneous carbonate with secondary carbonate, possibly by recrystallization in the presence of a hydrous fluid at very low temperature. Dolomite phenocrysts can be seen to be rimmed with fine-grained aggregates of brown secondary dolomite, which has completely pseudomorphed the mineral in some samples. Advanced alteration appears to involve replacement of even the secondary dolomite with calcite. Several samples with textures suggesting phytic dolomite have on anal-

ysis been shown to contain no Mg. Further field evidence for the presence of fluids occurs in the form of a ubiquitous network of veins and dykes of brown and yellow carbonate cross-cutting the sövites and alvikites, all of which show strong ^{18}O enrichment. The yellow carbonatite breccias also probably represent the products of fluidization, perhaps linked to surface eruption through an overlying volcanic edifice.

Much of the difference in $\delta^{18}\text{O}$ can be attributed to recrystallization of carbonate in response to equilibration with a hydrous fluid at temperatures $< 100^\circ\text{C}$. Such low temperatures would be required to provide the high fractionation of ^{18}O between carbonate and the fluid, which may have separated from the cooling carbonatite mass and migrated into veins and fractures. Direct precipitation from the fluid at low temperature is also likely, as evidenced by carbonate cementing the breccia pipes and the drusy vein fillings.

5.3. Variation in ^{13}C in the late-stage carbonate

The late-stage carbonate veins are all characterised by the highest $\delta^{18}\text{O}$ -values of $\sim +25\%$. Such high degrees of ^{18}O enrichment are most probably the result of equilibration with, and/or deposition from, hydrous fluids at low temperature ($< 100^\circ\text{C}$; Friedman and O'Neil, 1977). However, variation in $\delta^{13}\text{C}$ is quite marked, and several types of carbonate veins display strong depletion in ^{13}C . For the fluid to exert any control on $\delta^{13}\text{C}$, then it must contain species such as CO_2 and perhaps H_2CO_3 , as well as H_2O .

Variation in $\delta^{13}\text{C}$ in calcite deposited from a progressively degassing $\text{H}_2\text{O}-\text{CO}_2$ fluid could be achieved by varying several parameters such as: (1) the $\text{CO}_2/\text{H}_2\text{O}$ ratio; (2) the C-bearing species in the fluid (i.e. H_2CO_3 or HCO_3^-); and (3) the degree of equilibrium or Rayleigh fractionation. Zheng (1990) has modelled such

controls on carbon and oxygen isotope variation in carbonate precipitating from fluids. In order to produce carbonate strongly depleted in ^{13}C , relative to the main magmatic carbonatite complex that builds Dicker Willem, it would be necessary to propose Rayleigh-type fractionation of a fluid with X_{CO_2} of ~ 0.4 , at temperatures of $\sim 100^\circ\text{C}$. The dominant species in the fluid would have to be H_2CO_3 (as distinct from HCO_3^-), implying relatively low pH. Carbonates less depleted in ^{13}C would necessitate lower X_{CO_2} -values in the degassing fluid. Carbonates with $\delta^{13}\text{C}$ near zero would have to be deposited from fluids very poor in CO_2 .

6. Conclusions

The early intrusions of sövite, including calcite-phyric varieties, have carbon and oxygen isotope ratios similar to those for primary magmatic carbonatites (Taylor et al., 1967). Sövitites have average $\delta^{13}\text{C}$ of -5.0‰ and $\delta^{18}\text{O}$ of $+8.4\text{‰}$, compared with calcite phenocrysts with average $\delta^{13}\text{C}$ of -5.3‰ and $\delta^{18}\text{O}$ of $+7.3\text{‰}$. Interstitial carbonate in ijolite inclusions that occur within the sövitites, has average $\delta^{13}\text{C}$ of -5.0‰ and $\delta^{18}\text{O}$ of $+8.4\text{‰}$, and therefore shares the same carbon and oxygen composition as their host. This result taken together with the similar composition of silicate minerals, suggests that the sövitites and ijolites may represent the crystallized products of co-existing immiscible melt fractions.

The later alvikite intrusions are dolomite-phyric carbonatite magmas that were enriched in ^{13}C and ^{18}O by fractionation of a parental sövitic magma. Calcite and dolomite crystallizing from the fractionating carbonatite melt define a positive correlation between $\delta^{13}\text{C}$ and $\delta^{18}\text{O}$ (termed the phenocryst array), and produced carbonatites with $\delta^{13}\text{C}$ ranging from -5.5 to -3.4‰ and $\delta^{18}\text{O}$ from $+6.9$ to $+10.6\text{‰}$. Coprecipitation of silicates (Na-augite, biotite, nepheline, melanite), magnetite and apatite may also have contributed to the

observed enrichment in ^{18}O during differentiation. Bulk alvikites have $\delta^{13}\text{C}$ -values within the range of that observed for the phenocryst array, but have $\delta^{18}\text{O}$ -values that range up to $+18\text{‰}$. Such enrichment in ^{18}O is thought to be the product of post-magmatic recrystallization of primary carbonate in equilibrium with hydrous fluids at low temperatures. Such a process is confirmed by patterns observed in the late-stage carbonatite dykes and veins of carbonate, which possess very high $\delta^{18}\text{O}$ -values of $\sim +25\text{‰}$, indicative of equilibration with low-temperature fluids.

Acknowledgements

Support from the South African Foundation for Research Development (FRD) to D.L.R. and for a Visiting Fellowship to A.F.C. are gratefully acknowledged. Logistic support during field work was provided by Roy Miller of the Geological Survey of Namibia, Windhoek. Assistance provided by Chandra Mehl in the laboratory was invaluable. Melissa Kirkley assisted in the magnetite analyses. Andy Duncan suggested we tackle Dicker Willem. A.F.C. is grateful to the University of Otago for sabbatical leave. D.L.R. is grateful to the University of Cape Town for sabbatical leave and to the Universities of Tasmania and Otago for providing facilities during the completion of this paper.

References

- Bottinga, Y., 1968. Calculation of fractionation factors for carbon and oxygen isotope exchange in the system calcite-carbon dioxide-water. *J. Phys. Chem.*, 72: 800-808.
- Cooper, A.F., 1988. Geology of Dicker Willem, a subvolcanic carbonatite complex in south-west Africa. *Comm. Geol. Surv. S.W. Afr./Namibia*, 4: 3-12.
- Cooper, A.F. and Reid, D.L., 1991. Textural evidence for calcite carbonatite magmas, Dicker Willem, south-west Namibia. *Geology*, 19: 1193-1196.
- Dawson, J.B., 1989. Sodium carbonatite extrusions from Oldoinyo Lengai, Tanzania: implications for carbonate complex genesis. In: K. Bell (Editor), *Carbonate*

- tites: Genesis and Evolution. Unwin Hyman, London, pp. 255–277.
- Deines, P., 1989. Stable isotope variations in carbonatites. In: K. Bell (Editor), Carbonatites: Genesis and Evolution. Unwin Hyman, London, pp. 301–359.
- Deines, P. and Gold, D.P., 1973. The isotopic composition of carbonatite and kimberlite carbonates and their bearing on the isotopic composition of deepseated carbon. *Geochim. Cosmochim. Acta*, 37: 1709–1733.
- Ericksson, S.C., 1989. Phalaborwa: a saga of magmatism, metasomatism and miscibility. In: K. Bell (Editor), Carbonatites: Genesis and Evolution. Unwin Hyman, London, pp. 221–254.
- Fanelli, M.F., Cava, N. and Wyllie, P.J., 1986. Calcite and dolomite without portlandite at a new eutectic in $\text{CaO-MgO-CO}_2\text{-H}_2\text{O}$, with applications to carbonatites. In: Morphology and Phase Equilibria in Minerals. Proc. 13th Gen. Meet., Int. Mineral. Assoc., Bulgarian Acad. Sci., pp. 580–600.
- Friedman, I. and O'Neil, J.R., 1977. Compilation of stable isotope fractionation factors of geochemical interest. In: Data of Geochemistry. U.S. Geol. Surv., Prof. Pap. 440-KK, 6th ed., 107 pp.
- Gittins, J., 1989. The origin and evolution of carbonatite magmas. In: K. Bell (Editor), Carbonatites: Genesis and Evolution. Unwin Hyman, London, pp. 580–600.
- Hubberten, H.-W., Katz-Lehnert, K. and Keller, J., 1988. Carbon and oxygen isotope investigations in carbonatites and related rocks from the Kaiserstuhl, Germany. *Chem. Geol.*, 70: 257–274.
- Jackson, M.P.A., 1976. High grade metamorphism and migmatization of the Namaqua metamorphic complex around Aus in the southern Namib desert, South West Africa. *Bull. Precambrian Res. Unit, Univ. Cape Town*, 18, 299 pp.
- Janse, A.A., 1969. Gross Brukkaros, a probable carbonatite volcano in the Nama plateau of South West Africa. *Bull. Geol. Soc. Am.*, 80: 573–586.
- Knudsen, C. and Buchardt, B., 1991. Carbon and oxygen isotope composition of carbonates from the Qaqarsuk carbonatite complex, southern West Greenland. *Chem. Geol. (Isot. Geosci. Sect.)*, 86: 263–274.
- McCrea, J.M., 1950. On the isotopic chemistry of carbonates and a palaeotemperature scale. *J. Chem. Phys.*, 18: 849–857.
- Pineau, F., Javoy, M. and Allègre, C.J., 1973. Étude systématique des isotopes de l'oxygène, du carbone et du strontium dans les carbonatites. *Geochim. Cosmochim. Acta*, 37: 2363–2377.
- Reid, D.L., Cooper, A.F., Rex, D.C. and Harmer, R.E., 1990. Timing of post-Karoo alkaline magmatism in southern Namibia. *Geol. Mag.*, 127: 427–433.
- Sharma, T. and Clayton, R.N., 1965. Measurement of $^{18}\text{O}/^{16}\text{O}$ ratios of total oxygen of carbonatites. *Geochim. Cosmochim. Acta*, 29: 1347–1353.
- Suwa, K., Oana, S., Wada, H. and Osaki, S., 1975. Isotope chemistry and petrology of African carbonatites. *Phys. Chem. Earth*, 9: 735–745.
- Taylor, H.P., Frechen, J. and Degens, E.T., 1967. Oxygen and carbon isotope studies of carbonatites from the Laacher See district, West Germany, and the Alnö district, Sweden. *Geochim. Cosmochim. Acta*, 31: 407–430.
- Vennemann, T.W. and Smith, H.S., 1990. The rate and temperature of reaction of ClF_3 with silicate minerals, and their relevance to oxygen analysis. *Chem. Geol. (Isot. Geosci. Sect.)*, 86: 83–88.
- Verwoerd, W.J., 1966. South African carbonatites and their probable mode of origin. *Ann. Univ. Stellenbosch*, 41 (Ser. A2): 115–233.
- Zheng, Y.-F., 1990. Carbon–oxygen isotopic covariation in hydrothermal calcite during degassing of CO_2 . *Miner. Deposita*, 25: 246–250.